Journal of Alloys and Compounds 488 (2009) 112–116

Contents lists available at ScienceDirect

Journal of Alloys and Compounds

journal homepage: www.elsevier.com/locate/jallcom

Recrystallization of twin-roll cast Al–Fe–Si foil stock processed without homogenization

Yucel Birol*

Materials Institute, Marmara Research Center, TUBITAK, Kocaeli, Turkey

ARTICLE INFO

Article history:
Received 31 July 2009
Received in revised form 24 August 2009
Accepted 26 August 2009
Available online 1 September 2009

Keywords:
Thermomechanical processing
Differential scanning calorimetry
Aluminium alloys
Recrystallization

ABSTRACT

Differential scanning calorimetry, hardness testing, electrical conductivity measurements and microstructural analysis were employed in the present work to investigate the response of twin-roll cast Al–0.8Fe–0.6Si strips to interannealing without prior homogenization. Recrystallization which occurs at 400 °C in sheet samples cold rolled only lightly ($\varepsilon \sim 0.2$) is gradually displaced to lower temperatures with increasing strain until $\varepsilon \sim 2.3$. Precipitation occurs largely before a measurable recrystallization reaction at low strains, $\varepsilon < 2.3$, producing an acceptable grain structure across the section. The interaction of the two reactions at $\varepsilon > 2.3$ is believed to be responsible for a decreasing recrystallized fraction and for coarse grains at the surface where the interaction is likely to be most pronounced. Interannealing of the Al–0.8Fe–0.6Si alloy without a homogenization treatment produces acceptable grain structures across the section of the strip for much of the cold rolling strain range. It is thus concluded that Al–0.8Fe–0.6Si foil stock, intended for cosmetic foil applications where formability is not critical, could be processed without a high-temperature annealing treatment.

1. Introduction

Alloys from the ternary Al–Fe–Si system have been traditionally used as foil stock owing to a suitable combination of strength and formability at foil gauges [1]. The manufacturing cycle often starts with twin-roll casting and relies on a recrystallization anneal at some intermediate gauge to restore ductility to facilitate further rolling to foil gauges [2–5]. A relatively small volume of heat source and a relatively large heat sink in twin-roll casting lead to rapid solidification in the caster roll gap [6,7] producing cast strips in a non-equilibrium state. The softening kinetics in twin-roll cast (TRC) strips is generally slower with respect to the ingot-cast grades due to a finer dispersion of intermetallic particles and a higher level of matrix supersaturation [8–15]. The former provides a Zener drag while high solute levels can cause a strong solute-dislocation interaction during an annealing heat treatment [10,16,17].

TRC Al–Fe–Si strips are almost invariably submitted to a high-temperature anneal to allow the precipitation of excess Fe and Si in solution before further processing [2]. The primary function of such a high-temperature anneal in the case of TRC strips is to relax matrix supersaturation via precipitation, heterogenization rather than homogenization, owing to a dendritic structure already too fine to impair homogenity [6]. While it has a favorable impact on the recrystallization behaviour of Al–Mn [18,19], the homogenization step may not be necessary for Al–Fe–Si alloys [20]. This is particularly true for those alloys with a Si content nearly matching that of Fe. Si, known to be an effective Fe precipitator, acts to remove the solute Fe from the matrix during solidification. Differential scanning calorimetry (DSC), hardness testing, electrical conductivity measurements and microstructural analysis were employed in the present work to investigate the response of TRC Al–0.8Fe–0.6Si strips to interannealing without prior homogenization, with a particular emphasis on the evolution of the grain structure, a critical feature for most foil applications.

2. Experimental

100 mm × 100 mm pieces, sectioned from the centre of the TRC strip, cast industrially at a gauge of 6 mm with 0.81 wt.% Fe and 0.65 wt.% Si, were cold rolled using a fully instrumented laboratory rolling mill to achieve true strains between 0.2 and 3.7. The sheet samples thus obtained were submitted to annealing treatments between 250 °C and 550 °C in order to find out about their response to thermal exposure.

The TRC strip and cold rolled sheet samples were ground with SiC paper, polished with 3 μ diamond paste and finished with colloidal silica. Their microstructures were examined after etching with a 0.5% HF solution using a Olympus BX51M model optical microscope. The grain structures were investigated after anodic oxidation with Barker's solution, using cross polarizers. A Sigma Test Unit measured the electrical conductivity of the samples to estimate the extent of precipitation activities. Measures were taken to obtain reliable electrical conductivity data from the very thin foil samples produced by cold rolling to high true strain levels [19]. The foil samples were folded, over an area of 20 mm × 50 mm, repeatedly until a minimum thickness of 2 mm was obtained.

The XRD patterns were recorded with a Shimadzu XRD 6000 Diffractometer equipped with CuK_α radiation, at very low scanning rates to improve the counting

* Tel.: +90 262 6773084; fax: +90 262 6412309.
E-mail address: yucel.birol@mam.gov.tr.

0925-8388/$ – see front matter © 2009 Elsevier B.V. All rights reserved.
doi:10.1016/j.jallcom.2009.08.135

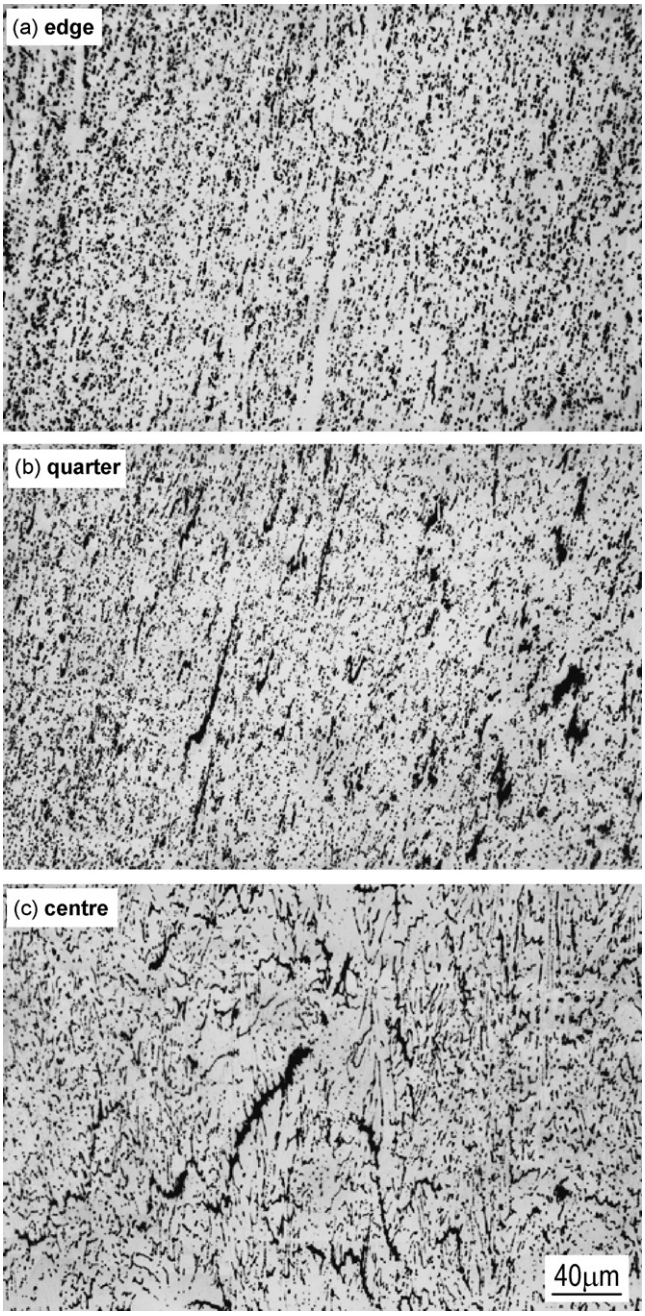

Fig. 1. Microstructure on the long transverse section of the TRC Al–0.8Fe–0.6Si alloy: (a) near the edge, (b) the quarter plane and (c) at the centre of the cast strip.

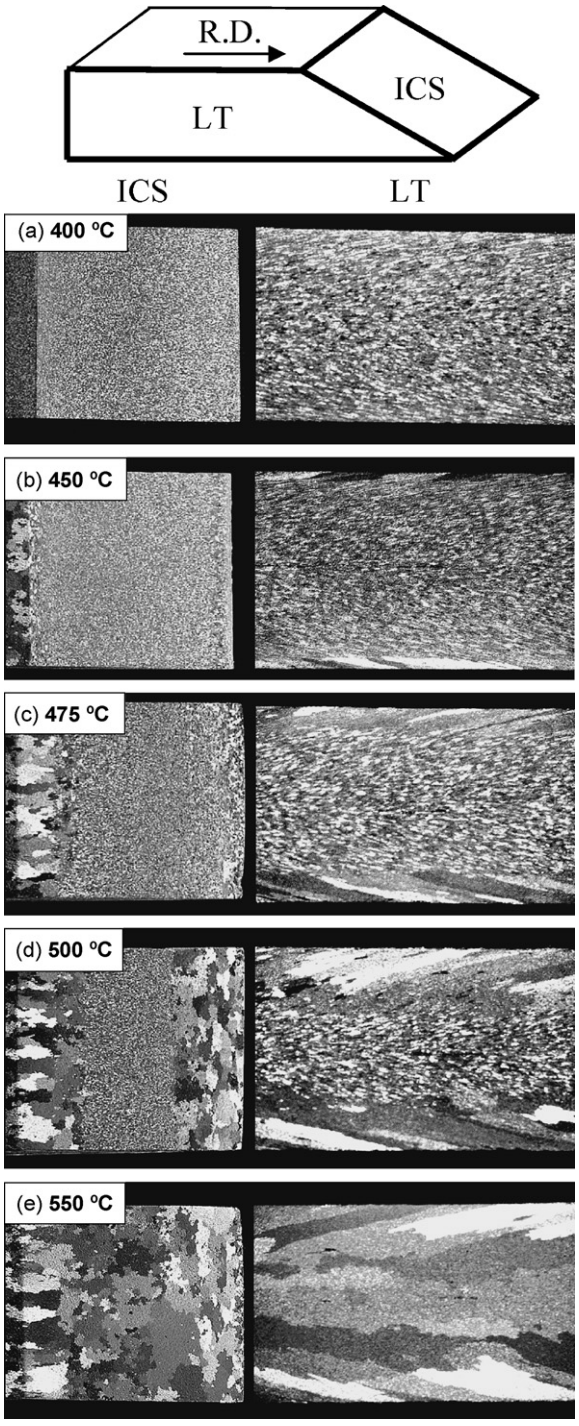

Fig. 2. Response of the TRC Al–0.8Fe–0.6Si alloy to a high-temperature annealing treatment: microstructures during heating at (a) 400 °C, (b) 450 °C, (c) 475 °C, (d) 500 °C and (e) 550 °C. LT: long transverse section; ICS: inclined cross section.

frequency. A JEOL JSM 5400 Scanning Electron Microscope (SEM) equipped with a Energy-Dispersive Spectroscopy (EDS) unit was also employed for the identification of intermetallic particles. Microhardness measurements were carried on transverse sections. The average of minimum 5 measurements was reported for the surface, quarter plane and the centre of the strip and processed sheet samples. Samples cold rolled to a strain of 3 and higher were too thin to allow hardness measurements at each of the three locations. Hardness only at the centre was thus reported for these samples.

3 mm diameter disc samples were gently machined from the cast strip and cold rolled sheet samples for DSC measurements. Runs were carried out at a heating rate of 10 K min^{-1} and under flowing argon (1 l h^{-1}) by placing the sample disc in the sample pan and super purity aluminium of equal mass in the reference pan of the cell. The heat effects associated with various reactions were then obtained by subtracting a super purity Al baseline run from a given heat flow curve. A second set of sheet samples, much larger in size than those used in the DSC tests was heated in an electric resistance furnace at the DSC scan rate and quenched from critical temperatures which mark the major enthalpic signals revealed in the DSC scans. These samples were then subjected to electrical conductivity and hardness measurements to identify the structural changes responsible for each of these signals.

3. Results and discussion

The microstructure of the TRC Al–0.8Fe–0.6Si strip (Fig. 1) was characterized by a fine dendritic network of α(Al) solid solution, typical of strip-cast alloys [21,22]. The gradual coarsening of structural features from the surface to the centre, typical of TRC strips, was noted as usual [6]. The dendrite arm spacing, measured to be

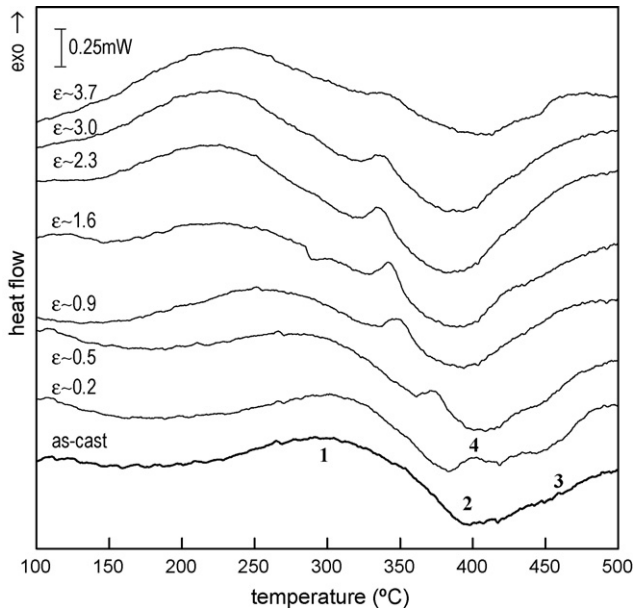

Fig. 3. DSC scans of the Al–0.8Fe–0.6Si cast strip and the sheet samples deformed by cold rolling to the indicated strain levels.

approximately 6 μ near the surface, was almost twice as large at the centre. The latter implies a cooling rate of 10^2 K s^{-1} [23] which is less than one-fifth of that experienced near the surface. The dendrite boundaries were decorated with intermetallic particles, the majority of which at the surface were identified by XRD and EDS to be of the monoclinic β-AlFeSi variety. Few particles revealed only a dominant Si peak and were thus identified as primary Si while a small fraction of the particles at the surface of the strip were judged to be the α-AlFeSi compounds with Fe/Si ratios exceeding 1.3. The centre of the strip revealed a similar distribution of intermetallic particles with β-AlFeSi still being the dominant phase. The cooling rate variation in this range seems to affect the scale of the dendritic structure and the size of the intermetallic particles but not their type.

The grain structure of the cast strip annealed without prior cold rolling is rearranged during annealing merely by a growth process above 450 °C with no evidence of recrystallization (Fig. 2). Grain growth starts at the surface and spreads across the section with increasing temperatures, producing coarse pancake shape grains

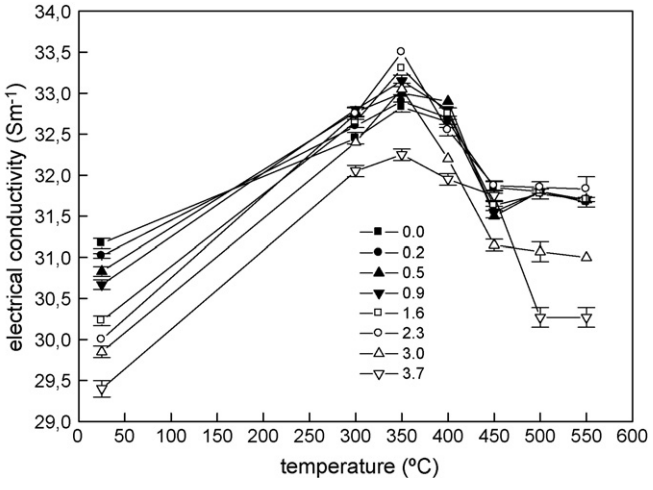

Fig. 4. Change with annealing temperature in the electrical conductivity of the Al–0.8Fe–0.6Si sheet samples deformed by cold rolling to the indicated strain levels.

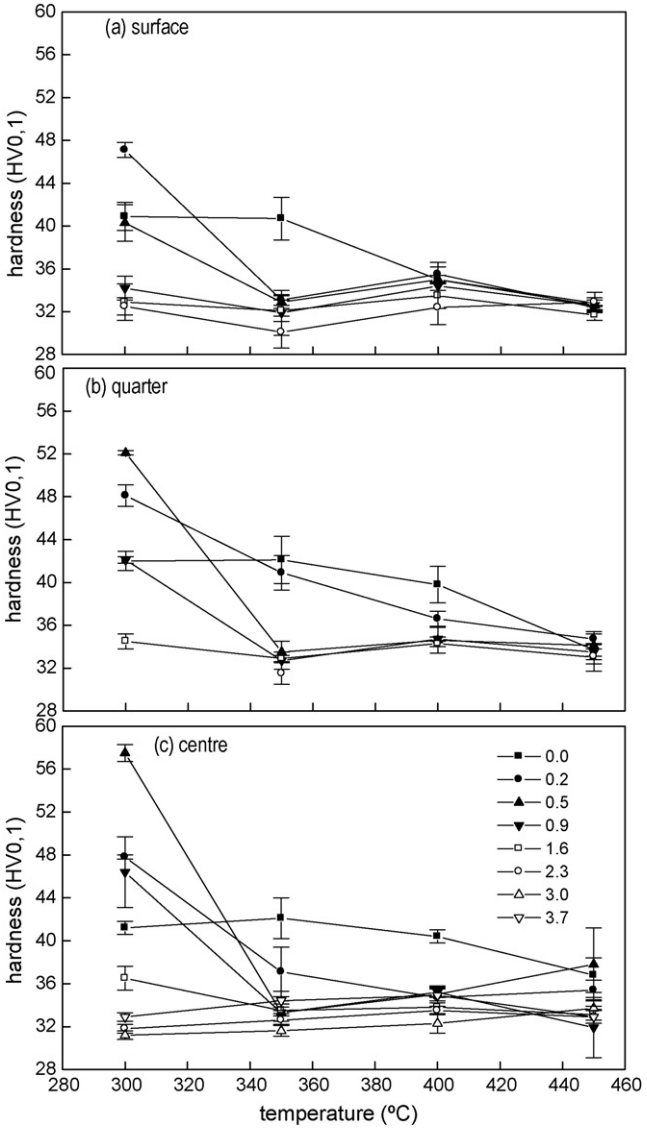

Fig. 5. Change with annealing temperature in the hardness of the Al–0.8Fe–0.6Si sheet samples deformed by cold rolling to the indicated strain levels. Hardness measurements were performed (a) near the surface (edge), (b) the quarter plane and (c) at the centre of the samples.

through the thickness starting at 450 °C. XRD analysis of cast strip samples submitted to a heating scan at 10 K min^{-1} until 550 °C has shown that the β-dominant as-cast structure is largely retained with slight changes in the intensity of the Si lines. This sequence is consistent with the DSC scan of the cast strip which reveals an exothermic peak centring around 300 °C (signal 1), a neighbouring endothermic trough at 400 °C (signal 2) and a final exothermic signal which extends beyond 500 °C (Fig. 3). The first of these signals is shown by electrical conductivity measurements to be associated with precipitation activities (Fig. 4). The electrical conductivity of the cast strip increases when annealed and peaks at 350 °C, right at the termination of signal 1, before levelling off above 450 °C. The precipitating species is likely to be Si which is known to be the major precipitating phase in all excess-Si aluminium alloys in this temperature range [24]. The endothermic trough which centres around 400 °C is claimed to be associated with the reversion of Si due to an increasing solid solubility. The last exothermic signal, signal 3, is attributed to grain growth, which, driven by the reduction of the total grain boundary energy, is indeed exothermic. Lack of recrystallization during annealing of the cast strip, in spite of

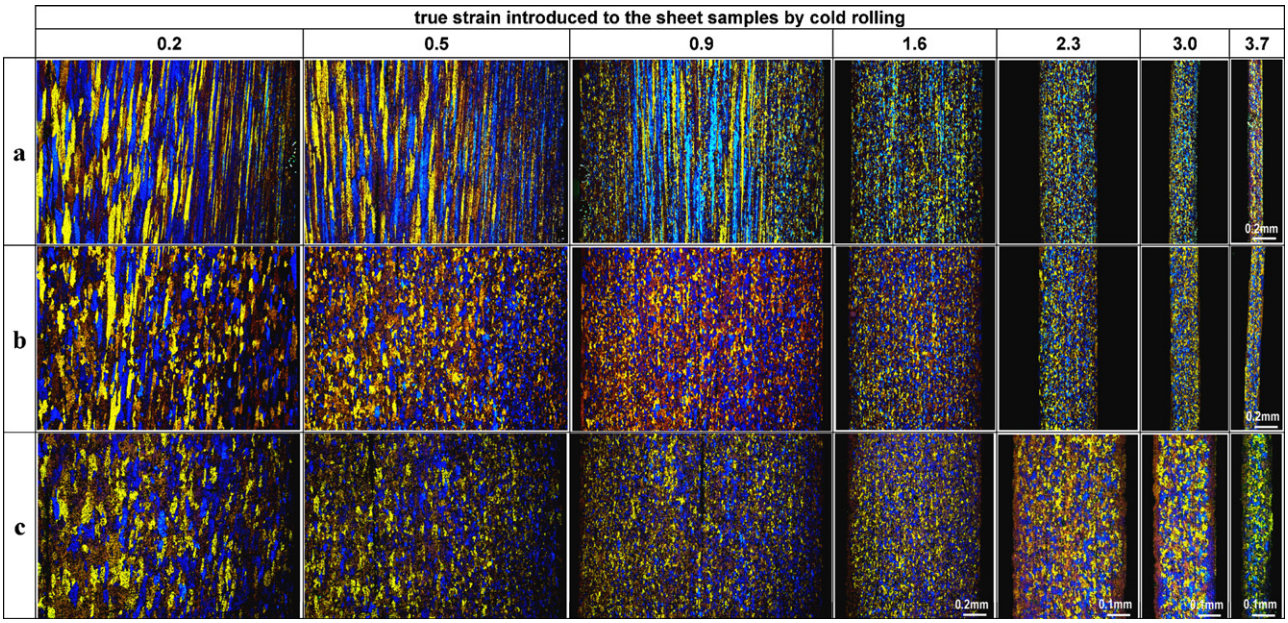

Fig. 6. Grain structures across the thickness of the Al–0.8Fe–0.6Si sheet samples cold rolled and subsequently submitted to annealing treatments at (a) 350 °C, (b) 400 °C and (c) 450 °C. The macrographs of the sheet samples cold rolled to $\varepsilon > 2.3$ and then annealed at 450 °C (the three at the bottom right corner) are taken at a magnification twice as high as the rest. The macrographs show only part of the sheet samples cold rolled to $\varepsilon < 0.9$.

some deformation inherited from the casting process, as inferred from the as-cast hardness, is evidenced also by through-thickness hardness measurements (Fig. 5). The cast strip fails to soften fully even at 450 °C.

The response to thermal exposure of the TRC Al–0.8Fe–0.6Si sheet samples cold rolled to a range of strains (ε) is illustrated with a series of DSC scans in Fig. 3. A small exothermic peak (signal 4) is superimposed on the DSC scan of the cast strip when it is cold rolled by $\varepsilon \sim 0.2$, before thermal exposure. Deformed grains, fully retained after annealing at 350 °C, are largely replaced by smaller equiaxed grains at 400 °C (Fig. 6). Signal 4 is thus readily identified as the recrystallization peak as it marks the onset of recrystallization at this strain level. Recrystallization at 400 °C after a cold rolling strain of only as much as $\varepsilon \sim 0.2$ is evidenced also by the through-thickness softening (Fig. 5). Unlike the cast strip, which retains its hardness after annealing at 400 °C, the hardness of sheet samples reduced in gauge by 20% ($\varepsilon \sim 0.2$) drops to soft temper level at 400 °C.

An increase in the strain to $\varepsilon \sim 0.5$ displaces the recrystallization peak to lower temperatures (Fig. 3), implying an improvement in recrystallization kinetics. In spite of a substantial displacement, the onset of the recrystallization peak is still above 350 °C and explains why sheet samples cold rolled to $\varepsilon \sim 0.5$ reveal no evidence of recrystallization at 350 °C (Fig. 6). Further increase in the strain level to $\varepsilon \sim 0.9$ displaces the recrystallization peak to around 350 °C. The recrystallization finish temperature, however, is still above 350 °C producing only a partially recrystallized sheet sample. Finally, a cold rolling strain of 1.6 allows nearly complete recrystallization at 350 °C for the first time (Fig. 6). Fibrous deformation grains in the centre of the strip that survive the annealing treatment at 350 °C after cold rolling to $\varepsilon \sim 0.9$, are now fully replaced by recrystallized grains. The recrystallization peak is gradually displaced to lower temperatures with increasing strain and grows bigger until $\varepsilon \sim 2.3$, due to an increase in the energy released during annealing sheet samples with higher strains. It apparently takes higher strains than 0.9 to produce fully recrystallized sheet samples at 350 °C (Fig. 6). It is clear from the foregoing that the cold rolled sheet samples fully recrystallize when annealed above, but not before, signal 4, regardless of the strain level. Hardness measurements provide further evidence for the recrystallization reaction claimed to be responsible for signal 4 (Fig. 5).

$\varepsilon \sim 2.3$ is the highest cold rolling strain that promotes the recrystallization reaction during a subsequent thermal exposure of the present alloy. Higher strains appear to have no favorable effect on the recrystallization reaction (Fig. 3). The shift of the recrystallization peak is in the opposite direction, to higher temperatures, in this high strain range and its size is gradually reduced with increasing cold rolling strains. Similar changes in the recrystallization peak features were noted in a supersaturated Al–Mn alloy and were accounted for by the prior recovery activity [18]. While the latter was evidenced in the Al–Mn alloy by a separate exothermic peak which grows with increasing strain, such a recovery peak is totally missing in the present alloy. The likelihood that the recovery peak is concealed by the enthalpic effect of the precipitation process, already very large at high strains, shall not be overlooked. The evolution of the precipitation peak itself could offer a plausible account of the marked change in the recrystallization peak features. The increase in size and in the temperature range of the precipitation peak at $\varepsilon > 2.3$ implies that the precipitation activities are dominating in a wide temperature range which extends beyond the recrystallization reaction in sheet samples cold rolled to $\varepsilon > 2.3$. Precipitation which occurs largely before a measurable recrystallization reaction at low strains is overlapping with the latter at $\varepsilon > 2.3$. Lack of an interaction between the precipitation and recrystallization reactions leads to an acceptable grain structure across the section of the annelaed sheet samples at $\varepsilon < 2.3$. The inevitable interaction of the two reactions at $\varepsilon > 2.3$, on the other hand, are believed to be responsible for a slightly decreasing recrystallized fraction and for the coarse grains at the surface where the interaction is likely to be most pronounced (Fig. 6).

4. Conclusions

It takes annealing temperatures as high as 400 °C to achieve recrystallization in Al–0.8Fe–0.6Si sheet samples cold rolled only lightly ($\varepsilon \sim 0.2$). The recrystallization reaction is gradually displaced to lower temperatures with increasing strain until $\varepsilon \sim 2.3$ which is the highest cold rolling strain that promotes the recrystallization

reaction. Precipitation occurs largely before a measurable recrystallization reaction at low strains, $\varepsilon < 2.3$, producing an acceptable grain structure across the section of the annelaed sheet. The inevitable interaction of the two reactions at $\varepsilon > 2.3$, on the other hand, is believed to be responsible for a slightly decreasing recrystallized fraction and for the coarse grains at the surface where the interaction is likely to be most pronounced.

Interannealing of the Al–0.8Fe–0.6Si alloy without a homogenization treatment produces acceptable grain structures across the section of the strip for much of the cold rolling strain range. It is thus concluded that Al–0.8Fe–0.6Si foil stock, intended for cosmetic foil applications where formability is not critical, could be processed without a high-temperature annealing treatment.

Acknowledgement

It is a pleasure to thank F. Alageyik for assisting in the experimental part of this work.

References

[1] P. Vangala, D. Smith, R. Duvvuri, C. Romanowski, in: E.F. Matthys (Ed.), Melt-Spinning and Strip Casting: Research and Implementation, The Minerals, Metals & Materials Society, Pennsylvania, 1992, pp. 225–262.
[2] Y. Birol, J. Mater. Process. Technol. 202 (2008) 564.
[3] K. Delijic, V. Asanovic, D. Radonjic, Mater. Sci. Forum 518 (2006) 543.
[4] Y. Birol, J. Alloys Compd. 458 (2008) 265.
[5] Y. Birol, J. Mater. Sci. 43 (2008) 4652.
[6] Y. Birol, M. Karlik, Prakt. Metallogr. 42 (2005) 325.
[7] Y. Birol, J. Mater. Process. Technol. 209 (2009) 506.
[8] M. Slamova, P. Slama, M. Cieslar, Mater. Sci. Forum 519–521 (2006) 365.
[9] S. Sarkar, M.A. Wells, W.J. Poole, Mater. Sci. Eng. A 421 (2006) 276.
[10] W.C. Liu, T. Zhai, J.G. Morris, Mater. Sci. Eng. A 358 (2003) 84.
[11] M. Koizumi, T. Saitou, H. Okudaira, H. Inagaki, Z. Metallkd. 91 (2000) 717.
[12] S. Tangen, K. SjØlstad, E. Nes, T. Furu, K. Marthinsen, Mater. Sci. Forum 396–402 (2002) 469.
[13] A.L. Dons, Z. Metallkd. 77 (1986) 126.
[14] C.J. Siemensen, R. Vellasamy, Z. Metallkd. 68 (1977) 428.
[15] M. Cieslar, M. Slamova, J. Uhlir, C. Coupeau, J. Bonneville:, Kovove Materialy-Metallic Mater. 45 (2007) 91.
[16] S. Benum, E. Nes, Acta Mater. 45 (1997) 4593.
[17] Y. Birol, J. Alloys Compd. 471 (2009) 122.
[18] Y. Birol, Scr. Mater. 59 (2008) 611.
[19] Y. Birol, Scr. Mater. 60 (2009) 5.
[20] Y. Birol, Scr. Mater. 61 (2009) 185.
[21] Y. Birol, Z. Metallkd. 89 (1998) 501.
[22] Y. Birol, F. Sertcelik, Z. Metallkd. 90 (1999) 329.
[23] H. Matyja, B.C. Giessen, N.J. Grant, J. Inst. Metals 96 (1968) 30.
[24] Y. Birol, J. Alloys Compd. doi:10.1016/j.jallcom.2009.05.043.